JOURNAL OF MATERIALS & CONSTRUCTION

JOURNAL OF VIETNAM INSTITUTE FOR BUILDING MATERIALS
ISSN 2734 - 9438 ISSN 1859 - 381X
Website: www.jomc.vn

Simulation of flexural behavior of FRP reinforced concrete beam

Nguyen B.Toan

[1] Department of civil engineering, Mien Trung university of civil engineering, 24 Nguyen Du st, Tuy Hoa city, Vietnam

KEYWORDS

Hybrid beam
tie contact
embedded
fracture energy
FRP reinforcement

ABSTRACT

This paper presents a finite element model which is considered the nonlinear material of the rebar steel, and concrete of the beam to investigate the behavior of fiber reinforced polymer (FRP) based on the commercial software ABAQUS. The different types of the constraint between steel rebar, FRP and concrete are also showed in this study. In our research, the sensitivity of the parameters such as mesh size, dilation angle, viscosity factor, and concrete fracture energy is also evaluated. These results in the current study are verified with the results obtained from the experiment which is conducted by the authors of the paper at the laboratory of Mien Trung university of civil engineering. The study figured out that using the solid bar element which is constrained with concrete by the embedded contact to simulate the FRP reinforced concrete beam is more optimized than applying the truss bar element. Another point is that based on the results of the current paper can be found the ways to adjust the simulation in ABAQUS that is suitable for the real beam.

1. Introduction

Reinforced concrete (RC) structures have used from the unrivaled dominance of steel over all other reinforcing materials for more than 100 years. However, this kind of material has revealed disadvantages such as insufficient concrete cover, poor concrete mix, and aggressive environments which can break down the protection layer and may lead to corrosion of the steel rebars. These destructive environments include marine surroundings, and the use of salt-contaminated aggregates in the concrete mixture. The effects of these problems need to be considered because of the unreliable durability of these structures as a result of corrosion of steel is a serious problem.

The solutions of the material for replacing steel rebars in reinforcement has been researched for a few decades, and FRP hybrid is one of the best ways for structural engineering to solve the disadvantages of steel rebars. Fiber reinforced polymer (FRP) composites were first used in the building industry during the late 1960s to construct all-composite buildings; the construction industry proposed that rebars for reinforcing concrete should be made from composite materials and prestressing tendons for concrete beams should also be manufactured from FRP composites at this time [1]. In a few recent decades, FRP has been increasingly used in civil infrastructure applications due to its advantageous properties such as high specific strength/ stiffness, light weight and corrosion resistance. The light weight of FRP provides significant savings in labor cost. Furthermore, fatigue durability and the transparency of FRP bars to magnetic and electrical fields makes them an applicable alternative to steel reinforcement in applications sensitive to electromagnetic fields such as magnetic resonance imaging [1].

Flexural behavior of hybrid FRP-concrete-steel rebars has been conducted by various researchers for many years. Flexural behavior is the best-understood aspect of FRP-reinforced concrete, with basic principles applying regardless of member configuration, reinforcement geometry, or material type. Two possible flexural failure modes prevail. Sections with smaller amounts of reinforcement fail by FRP tensile rupture, while larger amounts of reinforcement result in failure by crushing of the compression-zone concrete prior to the attainment of ultimate tensile strain in the outermost layer of FRP reinforcement [2].

Li and Wang [3] demonstrated that the GFRP rebars reinforcing engineered cementitious composite material improved terms of energy dissipation ratio, load-carrying capacity, shear resistance, crack width, and damage level. These findings provide preliminary insights into the interaction between the ductile matrix (in tension) and brittle reinforcement and are useful in improving the overall performance of FRP-reinforced structural elements. Many studies utilized analytical finite element modeling and/or experimental studies to investigate the behavior of reinforced concrete beams reinforced or strengthened with FRP. Aiello and Ombres [4] has conducted the experimental investigation that has been carried out on six concrete beams; one reinforced with only FRP rebars, one reinforced with only steel rebars, and four reinforced with a combination of FRP and steel rebars, and the analysis has also been carried out theoretically in the research. These authours showed that the increase of stiffness is more evident for beams reinforced with FRP rebars placed near the outer surface of the tensile zone and steel rebars placed at the inner level of the tensile zone, and in comparison with beams reinforced with only FRP rebars, the presence of steel reinforcement reduces crack width and crack spacing values. Gravina and Smith [5] have studied the flexural behaviour of indeterminate concrete beams reinforced with fiber reinforced polymer

https://doi.org/10.54772/jomc.v11i02.288

Received 12/04/2021, explanation 19/07/2021, Accepted 21/07/2021

(FRP) bars using a local deformation model whose results are compared with tests on simply supported and continuous concrete beams reinforced with FRP bars. This model can predict the flexural behavior, moment distribution and ductility of indeterminate FRP reinforced concrete beams under increasing load by modeling the progressive formation of flexural cracks, and the associated crack spacings and crack widths. El-Mogy et al. [6, 7] presented an experimental and a finite element study on the flexural behavior of continuous FRP-reinforced concrete beams. El-Mogy et al. [8] concluded that deflection can be decreased when increasing the transverse GFRP reinforcement in continuous concrete beams in spite of keeping the longitudinal reinforcement the same.

The current paper will examine how using the embedded contact is more beneficial than applying the tie contact for the constraint between steel rebars, FRP, and concrete by modeling a simplified concrete beam following the finite element method based on ABAQUS. This is the new point in our study in the simulation of the behavior and strength of concrete beams reinforced by hybrid steel and FRP bars. Moreover, the sensitivity of the material parameters of concrete will be also considered in this study to understand the significant effects of them on the results of modeling detailly.

2. Experimental program

2.1. Test set up and test procedure

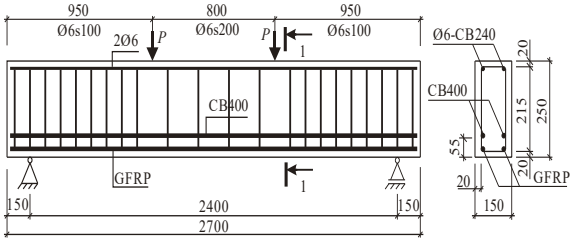

(a) Detail dimension and model for test

(b) The current experiment

Figure 1. Test set up.

Four-point flexural tests have been implemented using the arrangement shown in Figure. 1. The beam has been instrumented with a linear variable differential transducer (LVDT) at midspan to measure deflections. At the midspan, strain gauges have been bonded to the compression surface at different levels. The concrete tensile surface has been instrumented with an electrical displacement transducer to measure deformations.

In this test, the beam has been arranged in 2 bars diameter 14 FRP and 2 steel rebars diameter 14 in tension, 2 steel rebars diameter 6 in compression, the stirrup diameter for beam is 6, spacing hoop at the ends of the beam is 100 mm, and in the middle of the beam is 200 mm. The experiment carried out to investigate cracks, crushing, deformation as well as to know the load capacity of the beam. These results were to verify the results of modeling based on ABAQUS.

2.2. Materials properties

The model of concrete considered plastic damage in compression and tension was applied in this study [9]. For uniaxial compression and tension, the stress-strain relation under uniaxial loading in the damage-plasticity behavior displayed in Figure. 2, can be written as:

$$E = \left(1-d_c\right)E_0 \tag{1}$$

$$\sigma_c = \left(1-d_c\right)E_0\left(\varepsilon_c - \varepsilon_c^{pl}\right) \tag{2}$$

$$\sigma_t = \left(1-d_t\right)E_0\left(\varepsilon_t - \varepsilon_t^{pl}\right) \tag{3}$$

E is the is the reduced tangent stiffness and d is a scalar degradation variable, which is a function of stress state and of compression and tension damage variables (d_c and d_t, respectively). E_0 is the initial (undamaged) elastic stiffness (deformation modulus), and ε_{el} and ε_{pl} are the elastic (recoverable) and plastic (irrecoverable) strain, respectively.

The calculating of the damage variables starts from definition of compressive and tensile variables as the portion of normalized energy dissipated by damage:

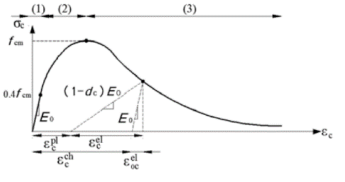

(a) Compression

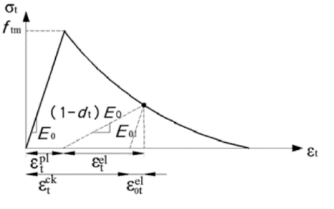

(b) Tension

Figure 2. Assumed uniaxial model of concrete behavior.

$$d_c = \frac{1}{g_c}\int_0^{\varepsilon_c^{ch}} \sigma_c d\varepsilon_c^{ch}; \qquad d_t = \frac{1}{g_t}\int_0^{\varepsilon_c^{ck}} \sigma_t d\varepsilon_c^{ck} \tag{4}$$

In the equation (4), ε_c^{ch} and ε_t^{ck} are the crushing and cracking strains respectively. The relationship stress and strain of concrete in compression and tension which were used in this study showed in Figure 4.

A bilinear relationship in hardening was used to represent the stress-strain curve of the steel reinforcement while a linear elastic behavior was used for the FRP rebars. The Poisson's ratio was assumed to be 0.3 for steel reinforcement and 0.2 for FRP. For stirrups, loading plates, and supporting plate the stress-strain relation were considered linear. Figure 7 shows the stress-strain relations of the different materials used. The material properties of the beam in this test were presented as detailed in Table 1.

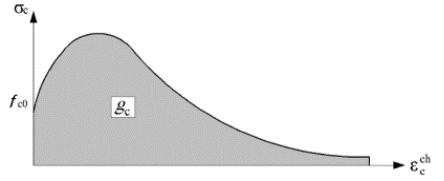

(a) Compression

(b) Tension

Figure 3. Parts of energy dissipated by damage.

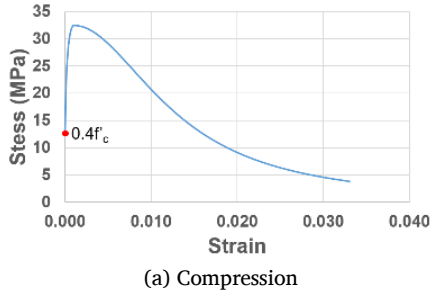

(a) Compression

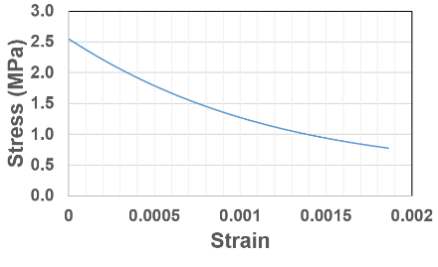

(b) Tension

Figure 4. Stress and strain curve for concrete.

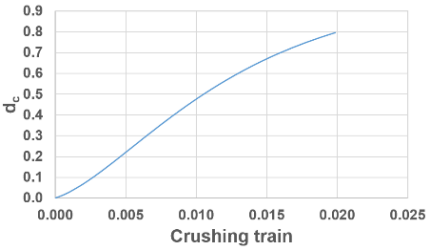

Figure 5. Relationship between compressive damage variable and crushing strain.

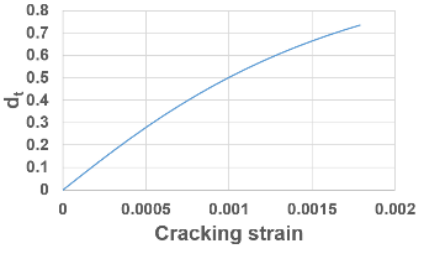

Figure 6. Relationship between tensile damage variable and cracking strain.

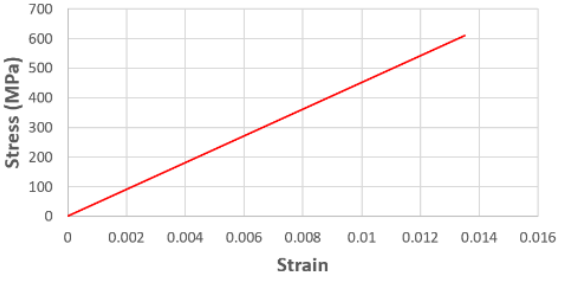

(a) FRP

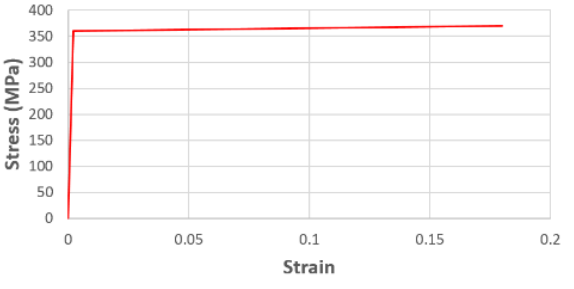

(b) Steel

Figure 7. Stress and strain curve for bars.

Figure 8. Fiber reinforced polymes.

3. Numerical simulation

In the current study, two nonlinear finite analysis models were implemented with the different types of the constraint of bars and concrete. In the first model, rebars, and FRP were constrained with concrete by embedded that was presented in Figure 10, and in the other model, the tie contact showed in Figure 11 was considered to investigate the beneficial simulation for hybrid FRP beam and can be applied to the model which obtains the adapted results for the other specimens in this experimental program to save computational time, but the results obtained is reasonable while changing the interaction between bars, stirrup, and concrete. The constraint between stirrup and concrete was assumed is embedded in both models which were showed in Figure 10 and Figure 12.

Table 1.

The details of material for beam.

Bottom reinforcement – FRP				
ϕ (mm)	Number of bars	f_u (MPa)	E (Gpa)	Poisson's ratio
14	2	610	45	0.2
Bottom reinforcement – steel				
ϕ (mm)	Number of bars	f_y (MPa)	E (Gpa)	Poisson's ratio
14	2	360	200	0.3
Top reinforcement – steel, stirrup				
ϕ (mm)	Number of bars	f_y (MPa)	E (Gpa)	Poisson's ratio
6	2	300	200	0.3
Concrete				
$f_c^{'}$ (MPa)	E (Gpa)	f_{tm} (MPa)	Poisson's ratio	
32.5	27	2.54	0.167	

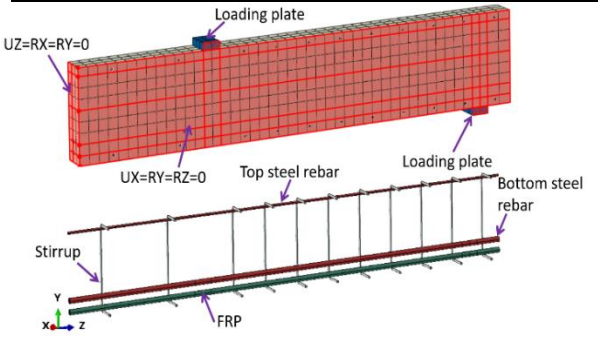

Figure 9. Finite element model for the beam.

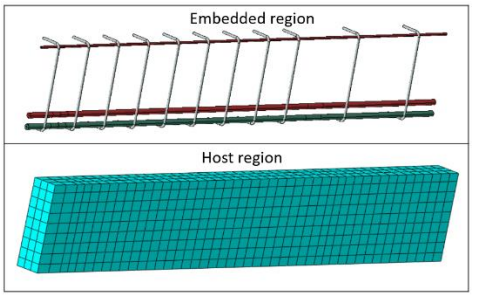

Figure 10. Defining constraint: Embedded region in the embedded model.

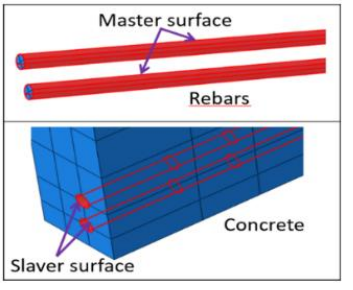

Figure 11. Tie contact between rebars and concrete in the tie model.

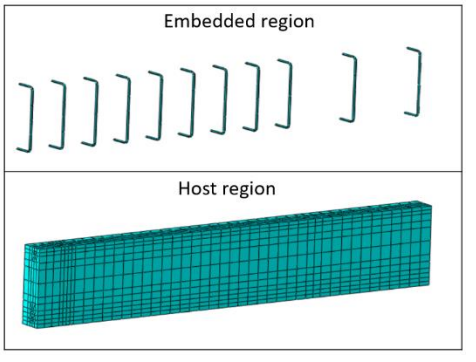

Figure 12. Defining constraint: Embedded region in the tie model.

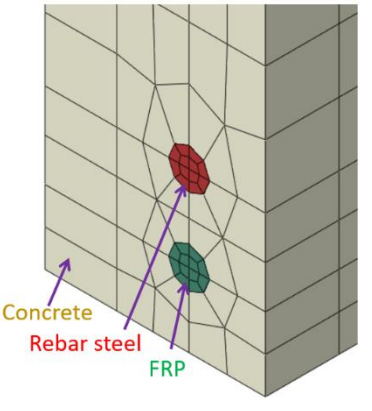

Figure 13. The mesh region of bars and concrete in the tie model.

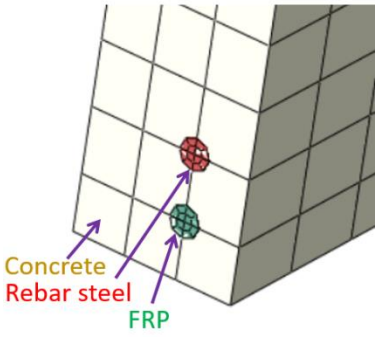

Figure 14. The mesh region of bars and concrete in the embedded model.

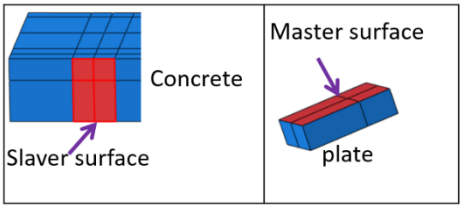

Figure 15. Tie contact between plates and concrete.

In the tied model, the surfaces of rebars steel, and FRP chose are master surfaces. The slaver surfaces were assigned on the surfaces of holes generated on concrete. To solve the convergence problem when using tie contact, the mesh was controlled how the region of nodes on the physical holes of concrete connected to nodes on the bars respectively. This means the common Degrees of Freedom (DoFs) are combined meaning that these nodes form pairs that have the same displacements and/or rotations. In the other model, the embedded model, the region of the embedded including rebars and FRP were hosted inside the concrete region. In that case, the physical holes in the concrete were not created. With this constraint, the DoFs of the nodes of the hosted beam will be connected with the DoFs of the nodes of the host beam that fall into a radius around the beam.

As shown in Figure 9, symmetries were used to model one fourth the specimen using the presented boundary conditions. In the first plane of symmetry, horizontal displacements in the Z direction, and rotations about the X and Y directions were restrained throughout the plane of symmetry. In the rest plane of symmetry, the horizontal degree of freedoms throughout the X direction, and rotations about the Y and Z directions were controlled. Displacements in the Y direction were also restrained along the centreline of the reaction plate. To simplify, the eight-noded reduced brick element (C3D8R) was applied to the whole model. A displacement control loading procedure was adopted. Steel reinforcement and structural steel materials were modeled using a bilinear elastoplastic model with strain hardening.

In order to accurately simulate the real behavior of the concerned beam, all its components; concrete beam, steel bars, FRP bars, and stirrups; have to be modeled properly. Meanwhile, choosing the element types, interaction, parameters of the materials, mesh size, and the compatibility of regions of mesh parts are important as well in the model to receive accurate results with reasonable computational time.

4. Results and analyzing

The results obtained from the observation of the load-deflection curve presented in Figure. 16 indicated that the similar tendency of the curve using the finite element method based on ABAQUS and the one from the experiment. The results implementing with the embedded model were more accurate than the curve based on the tie constraint between rebars, FRP, and concrete. According to the Figure 16, it can be seen that after the linear stage of concrete, the different behavior of the beam between the test and the tied model is significant. This can be explained that the displacements or/and rotations of elements on concrete are larger than strokes or/ and rotation of elements on the bars. However, in this model, tie constraint was applied, hence caused the considered difference. This figure also showed the ultimate load in test and ABAQUS based on the embedded model was approximate. Additionlly, the time computation of the embedded model was much faster than the time to obtain results by solving the tied model. According to the above things, the study can be concluded that using the embedded constraint between steel rebar, FRP, and concrete is reasonable to model the behavior of the hybrid beam for the other specimens in the testing program which was implemented at Mien Trung university of civil engineering as well as investigating the others result such as cracking and crushing.

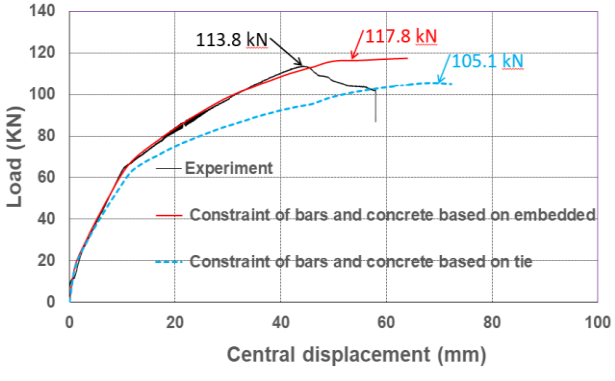

Figure 16. Load-deflection curve of the beam.

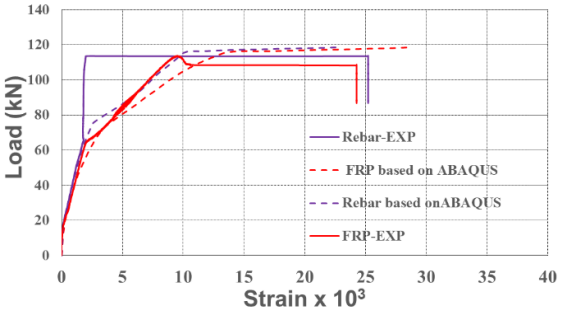

Figure 17. Relationship Load–Strain of FRP and rebar.

Combining the Figure 16 and Figure 17, it can be concluded that when the load reached 66.5 kN, or approximately 60 % the ultimate load, the FRP, and bottom rebars were yielded, strain was 0.002 respectively in neither bottom rebars nor FRP, the results also showed that the same point yielding in both test and ABAQUS. The similar load-strain curve between test and experiment based on FRP are also presented in Figure 17. However, there was the different bahavior of the bottom rebars after yielding while comparing between test and modeling, because in the test, strain gauge can not be bonded exact location where rebars were yielded. These are strong to ensure the reliable results of test and modeling in ABAQUS of our study.

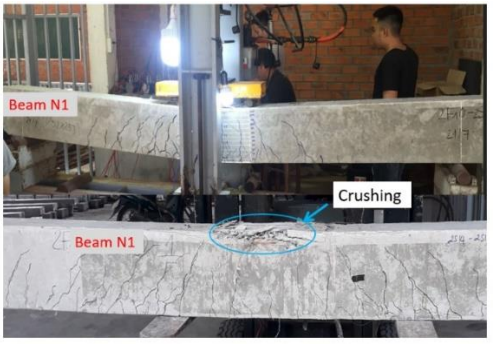

Figure 18. Cracking and crushing in the test.

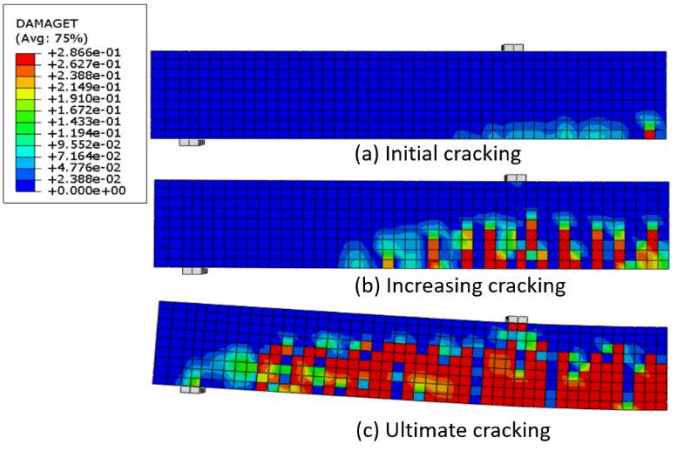

Figure 19. Generating and expanding cracking in the beam.

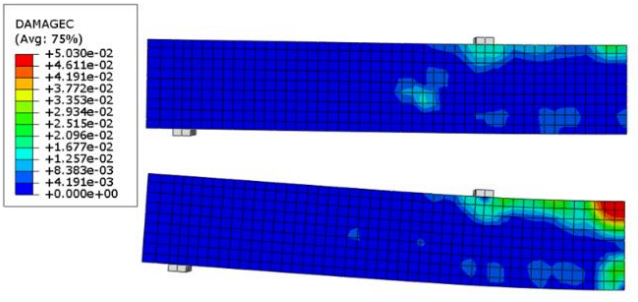

Figure 20. Crushing in the beam.

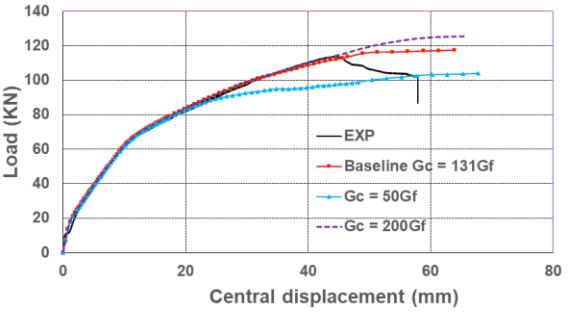

(a) Sensitivity of concrete fracture energy in compression

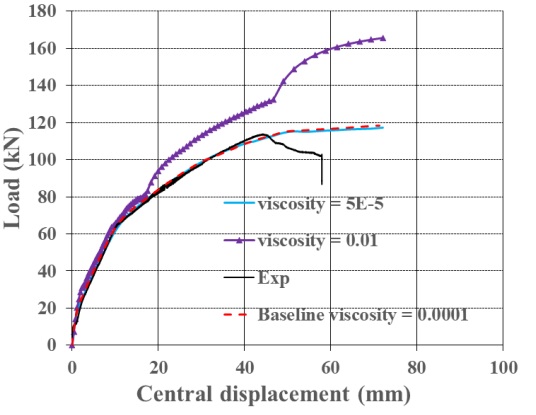

(b) Sensitivity of viscosity parameter

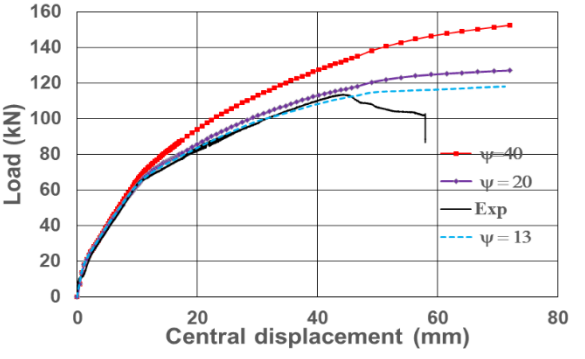

(c) Sensitivity of dilation angle

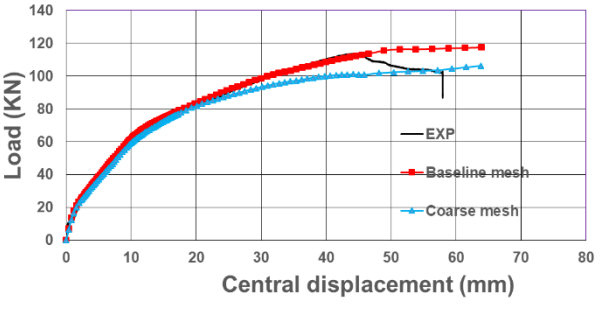

(d) Sensitivity of the mesh size

Figure 21. Sensitivity analysis of the beam.

From Figures. 18 to 20, showing the increment of cracking width and expanding the zone of cracking as well as the failure happened in the compression which might be realized in the analyzing the factor damage of concrete. The absence of plasticity in FRP materials implies that under reinforced flexural sections experience a sudden tensile rupture instead of a gradual yielding, as in the case of steel reinforcement. Thus, the concrete crushing failure mode of an over reinforced member is somewhat more desirable, due to enhanced energy absorption and greater deformability leading to a more gradual failure mode. Member recovery is essentially elastic with little or no energy dissipation resulting from large deformations. Another point from these figures is that based on tensile damage variable (DAMAGET) and compressive damage variable (DAMAGEC), the cracking and crushing of concrete were determined accurately. Detailing in the crushing and cracking region, the DAMAGEC factor is in around 0.05, the strain is 0.001, the DAMAGET factor is approximate 0.3, the strain is 0.0005 in compressive, tensile concrete respectively. This presents the suitability of the flexural behavior of concrete.

5. Conclusions

Using tie model in simulation of flexural behavior of FRP reinforced concrete beam is more accurate than embedded model. However, the tie model includes various elements and difficult constraints, so this model is not suitable for the main members such as concrete, plates…

This study ensures the reliable results of test and modeling in ABAQUS and developing in other large structures.

References

[1] L.C. Hollaway, Key Issues in the Use of Fibre Reinforced Polymer (FRP) Composites in the Rehabilitation and Retrofitting of Concrete Structures, Woodhead Publishing Limited, University of Surrey, UK, 2011.

[2] Bakis CE, Bank LC, Brown VL, Cosenza E, Davalos JF, Lesko JJ, et al. Fibre-reinforced polymer composites for construction: State-of-the Art review. Journal of Composites Construction, ASCE 2002;6(2):73–87.

[3] Li, V.C., and Wang, S., “Flexural Behaviors of Glass Fiber-Reinforced Polymer (GFRP) Reinforced Engineered Cementitious Composite Beams,” ACI Materials Journal Vol. 99, No. 1, January-February 2002, pp. 11-21.

[4] Aiello MA, Ombres L. Structural performances of concrete beams with hybrid (fiber reinforced polymer-steel) reinforcements. J Compos Constr, ASCE 2002; 6(2):133–40.

[5] Gravina RJ, Smith ST. Flexural behaviour of indeterminate concrete beams with FRP bars. Eng Struct 2008;30(9):2370–80.

[6] M. El-Mogy, A. El-Ragaby, E. El-Salakawy, Flexural behavior of continuous FRP-reinforced concrete beams, J. Compos. Constr. 14 (6) (2010) 669–680.

[7] M. El-Mogy, A. El-Ragaby, E. El-Salakawy, Experimental testing and finite element modeling on continuous concrete beams reinforced with fibre reinforced polymer bars and stirrups, Can. J. Civ. Eng. 40 (2013) 1091–1102.

[8] M. El-Mogy, A. El-Ragaby, E. El-Salakawy, Effect of transverse reinforcement on the flexural behavior of continuous concrete beams reinforced with FRP, J. Compos. Constr. 14 (6) (2011) 672–681.

[9] Alfarah B, López-Almansa F, Oller S. New methodology for calculating damage variables evolution in plastic damage model for RC structures. Engineering Structures (published online). 2017.